◆ Human Brain Mapping 38:1532–1540 (2017) ◆

Microstructural Changes of Brain in Patients with Aromatic L-Amino Acid Decarboxylase Deficiency

Wang-Tso Lee,[1,2]* Jui-Hsiang Lin,[3] Wen-Chin Weng,[1,2] and Steven Shinn-Forng Peng[2,4]*

[1]Department of Pediatrics, National Taiwan University Hospital and National Taiwan University College of Medicine, Taipei, Taiwan
[2]Clinical Center for Neuroscience and Behavioral Medicines, National Taiwan University Hospital, Taipei, Taiwan
[3]Institute of Epidemiology and Preventive Medicine in the College of Public Health, National Taiwan University, Taipei, Taiwan
[4]Department of Radiology, National Taiwan University Hospital and National Taiwan University College of Medicine, Taipei, Taiwan

Abstract: Aromatic L-amino acid decarboxylase (AADC) deficiency is an uncommon inherited neurometabolic disease. The clinical presentations and MR findings in children with AADC deficiency were investigated. Total 12 children (6 boys, 6 girls), aged from 9 to 50 months (mean, 23 ±13 months), with AADC deficiency, were enrolled for analysis. Of 12 patients enrolled, clinical presentations included global developmental delay with generalized hypotonia in 12 (100%), dystonia in 12 (100%), oculogyric crisis in 12 (100%), and excessive sweating in 8 (67%). Sleep problem was also found in 4 (33%). Of 15 MR examinations, the major changes included 6 (40%) with diffusely prominent bilateral frontal sulci, 10 (67%) with prominent frontal horns, and 12 (80%) with hypomyelination. In AADC patients, the frontal horn was significantly widened ($P < 0.01$), and the volume of caudate nucleus was also significantly smaller than that of controls ($P = 0.02$). The ratios of thickness of the splenium to that of the genu of corpus callosum were also significantly increased ($P < 0.01$). There was also significant decrease of fiber density indices in major white matter fiber tracts. Using Tract-Based Spatial Statistics approach, we also revealed significant change in major fiber tracts related to language function and motor function. In conclusion, the present study indicated that AADC deficiency may have significant impact on brain development, especially the frontal lobe and fiber tracts related to language function and motor function. Long-term follow-up of brain MRI in patients with AADC deficiency may clarify the possible effect of AADC deficiency on brain development. *Hum Brain Mapp 38:1532–1540, 2017.* **© 2016 Wiley Periodicals, Inc.**

Key words: magnetic resonance image; diffusion tensor imaging; brain; aromatic L-amino acid decarboxylase deficiency; children

*Correspondence to: Wang-Tso Lee; Department of Pediatrics, National Taiwan University Hospital, 7 Chung-Shan South Road, Taipei 100, Taiwan. E-mail: leeped@hotmail.com OR Steven Shinn-Forng Peng; Department of Radiology, National Taiwan University Hospital, 7 Chung-Shan South Road, Taipei 100, Taiwan. E-mail: steven0131@mail2000.com.tw
Financial Disclosure/Conflict of Interest: no disclosure or conflict of interest.

Funding sources: none.

Received for publication 5 April 2016; Revised 30 September 2016; Accepted 6 November 2016.

DOI: 10.1002/hbm.23470

Published online 17 November 2016 in Wiley Online Library (wileyonlinelibrary.com).

INTRODUCTION

Aromatic L-amino acid decarboxylase (AADC) deficiency is an uncommon neurometabolic disorder in children [Lee et al., 2009a,b]. AADC deficiency is more prevalent in Taiwan than that in western countries. The AADC patients in Taiwan mostly have IVS6 + 4A>T mutation, and it may have founder effect [Lee et al., 2009b]. Patients with AADC deficiency usually present with developmental delay, generalized hypotonia, and severe movement disorders like paroxysmal dystonia and oculogyric crisis [Brun et al., 2010; Hsieh et al., 2005; Lee et al., 2009a; Pons et al., 2004]. There is also no speech for most patients with AADC deficiency. However, the response to the treatment and the long-term effect of AADC deficiency on brain development remains unclear. Because AADC plays an important role in the synthesis of monoamines, including dopamine, serotonin, and other catecholamines, and all monoamines had widespread distribution in the brain [Brun et al., 2010; Hsieh et al., 2005; Lee et al., 2009a, b; Pons et al., 2004], deficiency of AADC may result in the abnormal development of the brain [Shih et al., 2013].

Magnetic resonance (MR) imaging, including diffusion tensor imaging (DTI), is a noninvasive neuroimaging modality to disclose the structural changes of the brain in different neurological disorders, including the neurometabolic disorders [Lee et al., 2009b; p. 4]. Several quantitative diffusion parameters are frequently used in DTI to evaluate the white matter fiber tracts in these disorders, including: (1) fractional anisotropy (FA), which reflects the water diffusion and coherence in fiber tracts; (2) axial diffusivity, measuring the magnitude of diffusivity along the direction of fiber tracts; and (3) radial diffusivity, measuring the magnitude of diffusivity perpendicular to the fiber tracts. Recently, fiber density index (FDI) had been introduced as a measure to quantify white matter fiber attenuation [Roberts et al., 2005; Ukmar et al., 2012]. The FDI correlates well with reduced FA, and could be combined with FA to offer an improved description of pathologies in white matter.

Either voxel-based statistics (VBS) or Tract-Based Spatial Statistics (TBSS) approaches have been used to analyze FA changes in different fiber tracts [Jovicich et al., 2014; Fan et al., 2016; Smith et al., 2006]. VBS of FA images has preserved the complete white matter structure and can be used to compare FA of different fiber tracts in corresponding areas. However, the FA differences in some voxels using VBS approach may arise from differences in the local morphometry in different patients rather than from microstructural differences. Therefore, the observer-independent TBSS approach, which retains the advantage of VBS and can better reflect the FA changes of microstructure in white matter, has been applied to evaluate the fiber tract integrity in different neurological diseases in recent years.

Most previous studies in patients with AADC deficiency have described unremarkable MR findings [Brun et al., 2010; Lee et al., 2009a, b; Pons et al., 2004]. Previous reports of PET findings have also shown decreased 18F-Dopa uptake mainly at both frontal areas and corpus striatum [Hsieh et al., 2005], indicating the impact of AADC deficiency is more severe over frontal cortex. However, there was no study evaluating white matter fiber tracts in patients with AADC in the past. Therefore, in the present study, we explore the findings on MR images of patients with AADC deficiency using conventional and TBSS approach, especially at the frontal lobe and corpus striatum, to investigate the relationship between MR findings and clinical presentations.

MATERIALS AND METHODS

We enrolled 12 patients (6 boys, 6 girls), aged from 9 to 50 months (mean, 23 ± 13 months), with AADC deficiency diagnosed by clinical presentations, CSF neurotransmitter measurements, and mutation analysis. 18F-Dopa PET was also performed in most cases to confirm the diagnosis [Lee et al., 2009a]. The clinical presentations, severity of neurological symptoms, and electroencephalography findings were evaluated by the child neurologist. Neuroimages were done after the diagnosis of AADC deficiency before the initiation of treatment, and the findings were evaluated by a neuroradiologist without knowing the clinical manifestations. Total 15 MR examinations, including three follow-up studies, were enrolled for evaluation.

The control group included another 15 age- and sex-matched unrelated subjects (mean age, 23 ± 13 months) were also referred to MR examinations for headache (11 patients), a scalp mass (2 patients), and localized neck hemangiomas (2 patients). Age difference between the study and control groups was not larger than 2 months. All patients in the control group have normal neurological development, and are free of neurological deficits evaluated by child neurologists.

The institutional ethic committee of National Taiwan university Hospital approved the present study. All patients and control subject received MR examinations using a 1.5-T echo-planar scanner (Sonata; Siemens, Erlangen, Germany). All MR examinations used a standard birdcage head coil in a 1.5-T MR system (Sonata; Siemens, Erlangen, Germany). At first, fast spin-echo (FSE) T2-weighted images (T2WIs) in the axial plane were obtained with TR/TE = 4,330/100 ms, echo train length = 11, matrix size = 256 × 256, field of view = 14 × 14 to 20 × 20, slice thickness = 4–5 mm with gap of 1–1.5 mm, and one acquisition. FSE T1-weighted images in the axial plane were then obtained, with TR/TE = 600–750/20 ms, matrix size = 256 × 256, field of view = 14 × 14 to 20 × 20 s, slice thickness = 4–5 mm with gap of 1–1.5 mm, and one acquisition. At last, FSE T2WIs were also performed in the sagittal plane with TR/TE = 5,360/100 ms, echo train length = 11, matrix size = 256 × 256, field of view = 14 × 14 to 20 × 20 s, slice thickness = 2 mm without gap, and

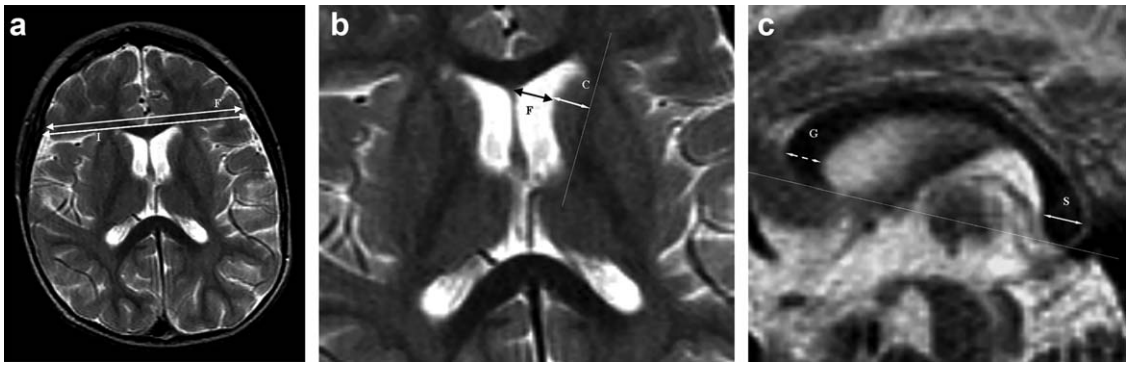

Figure 1.
FSE T2WI of a 23-month-old girl with AADC deficiency showing the FI ratios (a), the FC ratios (b), and SG ratios (c).

two acquisitions. DTIs were acquired using diffusion encoding gradients along 41 directions, and diffusion sensitivity b = 1,000 s/mm^2. The imaging parameters included TR/TE = 240/124 ms, matrix size = 128 × 128, field of view = 14 × 14 to 20 × 20 s, slice thickness = 4 mm without gap, and one acquisition. Follow-up MR examinations were done in 3 of 12 patients at the age of 22, 36, and 38 months, respectively.

Since T1-weighted image was the tool used in assessing myelination during the first 6 months of age [Yamada et al., 2000], the myelination milestones were determined by T1-weighted images for patients younger than 6 months, and by T2WIs when patients reached 6 months [Barkovich et al., 1988].

In all patients and control subjects, ratios of the transverse diameter of both frontal lobes to the distance between inner tables of both frontal calvarium (FI ratios) were measured along the right-left axis of the genu of the corpus callosum (Fig. 1a). Ratios of the thickness of the left frontal horn to the caudate nucleus (FC ratios) were also calculated along an axis perpendicular to the anterior limb of the left internal capsule on the axial FSE T2WIs (Fig. 1b). On the paramedian sagittal FSE T2WIs, ratios of the thickness of the splenium to that of the genu of the corpus callosum (SG ratios) were also obtained (Fig. 1c). The volume of the left caudate nucleus was measured by adding the products of slice thickness and the areas of regions of interest drawn by free hand on sagittal FSE images.

Image Processing

The structural data of DTIs were passed through the software of FSL software (http://www.fmrib.ox.ac.uk/fsl/index.html, FMRIB Software Library, Release 4.1 2008, The University of Oxford) Brain Extraction Tool was used to extract the diffusion-related signals of the brain [Smith et al., 2004; Woolrich et al., 2009]. After correcting eddy current-induced image distortions, all the DTIs were fit into the diffusion tensor model using FMRIB's Diffusion Toolbox (FDT). The FA data from FDT were then aligned by a nonlinear three-dimensional warp, aligning all FA images to those of a pre-defined, representative control subject, whose FA images had already affine-aligned with a 1 × 1 × 1 mm MNI152 standard space, providing in-plane and through-plane alignment [Smith et al., 2004]. On a voxel-by-voxel basis, fractional anisotropy and apparent diffusion coefficient, the latter decomposed into its 1st, 2nd, and 3rd eigen value components, were computed using FDT. FDI was computed for each voxel in selected areas as the total number of reconstructed fibers penetrating that voxel using the DTI studio tool 2.4 from the John Hopkins University Hospital [Jiang et al., 2006; Roberts et al., 2005].

To achieve common anatomical coordinates across patients, a fractional anisotropy template was constructed from a control subject selected by TBSS and affine-aligned into MNI152 standard space, fractional anisotropy data of all controls and AADC patients was also transformed with group-wise affine registration. The fractional anisotropy (FA) between the AADC and control groups was compared by TBSS analysis corrected for multiple comparisons using threshold-free cluster enhancement (TFCE). Region-of-interest (ROI) method was, then, applied to those regions with significant difference according to TFCE comparisons to measure the apparent diffusion coefficient (ADC), FA, $\lambda 1$, $\lambda 2$, and $\lambda 3$.

Fiber Tracking

A more detailed description of our fiber tracking procedures appears elsewhere [Xu et al., 2002]. The fiber tracking applies a target–source convention [Behrens et al., 2007]. Fiber tracking bundle targets were identified on the fractional anisotropy template in white matter regions with significant difference of FA. Tracking parameters specified minimum fractional anisotropy (0.15), 30° maximum angular deviation between voxels, and minimum (11.25 mm) and maximum (45 mm) fiber lengths, with

essentially no limit on the number of fibers. We refer hereafter to the group of fibers coursing through each target region as "fiber bundles."

Statistical Analysis

The difference of neuroimage indices between the AADC patients and control subjects were assessed with Mann–Whitney nonparametric analyses. Bonferroni-adjusted P value was used to perform multiple comparisons for fiber density index and DTI changes. The significance level was set to $\alpha = 0.05$.

RESULTS

Demographic Data

The diagnosis of AADC deficiency was based on the neurological symptoms, mutational analysis and change of CSF neurotransmitters, including low homovanillic acid and 5-hydroxyindoleacetic acid, and elevation of 3-ortho-methyldopa and levodopa. Of 12 patients enrolled, clinical presentations included global developmental delay with generalized hypotonia in 12 (100%), dystonia in 12 (100%), oculogyric crisis in 12 (100%), and excessive sweating in 8 (67%). Sleep problem (sleep apnea) was also found in 4 (33%) (Table I). The patients with AADC deficiency always have dystonia, which may be paroxysmal, and last for minutes to hours. Generalized dystonia sometimes was more severe in older children. Younger infants tend to have paroxysmal dystonia. About language development, five patients (6 months in one, 7 months in one, 9 months in two, and 15 months in one) only had cooing, and did not have babbling in speech. For those over 12 months old, no one can speak words or phrases with significant meaning. Only seven of eight patients can speak babbling. One 15-month-old girl suffered from focal seizures. About the mutation analysis, eight patients had IVS6 + 4A>T homozygous mutations, three had IVS6 + 4A>T heterozygous mutation, and one had c1298-1299InsA heterozygous mutation. Eight patients had ^{18}FDOPA-PET examination, and only one revealed trace uptake in striatal area. The patient with trace uptake in striatal area had CSF neurotransmitter confirmation of AADC deficiency. The HVA and 5-HIAA were below the detection level. The level of 3-o-MD was 961 nM, and the level of L-dopa was 64.6 nM. Both were above the normal range. The clinical presentation of the patient was also compatible with the diagnosis of AADC deficiency. EEG was performed in all patients, and the major change in EEG was mildly slow background activity without epileptiform discharges, indicating seizures were not common in these patients.

Conventional Neuroimaging Evaluation

Of 15 MR examinations, the major changes of magnetic resonance imaging (MRI) included 6 (40%) with diffusely prominent bilateral frontal sulci and subarachnoid spaces, 10 (67%) with prominent both frontal horns, and 12 (80%) with hypomyelination or changes in periventricular white matters. For clarification of myelination in patients, T2-weighted images (T2WIs) of all patients were compared with the T2WIs on the atlas of myelination [Barkovich, 2000; Schiffmann and van der Knaap, 2009]. Patients with a white matter region of higher signal intensity on T2WIs than those shown on the age-matched T2WIs on the atlas were considered hypomyelination at the white matter region [Schiffmann and van der Knaap, 2009]. In one patient, thin corpus callosum, mainly disclosed at the genu part, was also evident. Three patients had prominent choroid fissures. In addition, subdural fluid overlying the right frontal lobe was revealed in one patient, who also had prominent bilateral frontal sulci.

Although there was no significant difference in FI ratio, the frontal horn was significantly widened in the AADC patients than that of the controls ($P < 0.01$), and the volume of the caudate nucleus was also significantly smaller than that of controls ($P = 0.02$), leading to significant increase of the FC ratios in AADC patients compared with those in controls ($P < 0.01$) (Table II). The SG ratios were also significantly increased in patients with AADC deficiency ($P < 0.01$), indicating more significant atrophy at the genu of corpus callosum.

In the three patients with follow-up MR examinations at 11, 15, and 21 months later, respectively, two had mildly increased signal intensity in substantia nigra; all revealed progressive mesiotemporal atrophy, including hippocampus, amygdala, and parahippocampal gyrus, and decrease of subcortical and periventricular white matters. Although the volume of the caudate nucleus increased from 2.15 and 1.76 cm^3 to 2.92 and 2.02 cm^3, respectively, in two patients, the volume of the caudate nucleus in one patient decreased from 2.85 to 1.94 cm^3, and the frontal horn increased from 0.71 to 0.82 cm, indicating mildly progressive cerebral atrophy was possible in AADC deficiency.

Fiber Density Index and DTI Changes

For evaluation of fiber density, voxel-based statistics were used, which revealed significantly decreased FDI in most major fiber tracts. After Bonferroni correction, the most significant difference can be found in cerebellar white matter (8.41 ± 4.32 vs. 13.45 ± 4.09, Bonferroni-adjusted P value <0.01), frontostriatal white matter (6.69 ± 4.07 vs. 12.92 ± 3.53, Bonferroni-adjusted P value <0.01), posterior limb of the internal capsule (9.35 ± 5.72 vs. 12.69 ± 4.12, Bonferroni-adjusted P value <0.05), and superior longitudinal fasciculus (10.20 ± 6.80 vs. 16.09 ± 7.53, Bonferroni-adjusted P value <0.05). The FDI in frontal white matter was more significantly decreased compared with other areas, compatible with the findings in conventional MRI.

TABLE I. Clinical manifestations and mutational analysis in patients with AADC deficiency

Case	Age at diagnosis (month)	Sex	Clinical manifestations	Mutational analysis	Uptake of striatum in ^{18}FDOPA-PET
1	6	M	Psychomotor retardation, generalized hypotonia, paroxysmal dystonia, oculogyric crisis, excessive sweating, no babbling, or cooing	IVS6 + 4A>T/IVS6 + 4A>T	No uptake
2	7	M	Developmental delay, generalized hypotonia, paroxysmal dystonia, oculogyric crisis, excessive sweating, no babbling, only cooing	IVS6 + 4A>T/IVS6 + 4A>T	No uptake
3	9	F	Developmental delay, generalized hypotonia, paroxysmal dystonia, oculogyric crisis, excessive sweating, no babbling, only cooing	IVS6 + 4A>T/c1298-1299InsA	Not done
4	9	F	Developmental delay, generalized hypotonia, paroxysmal dystonia, oculogyric crisis, sleep problem, excessive sweating, no babbling, only cooing	IVS6 + 4A>T/IVS6 + 4A>T	No uptake
5	12	F	Developmental delay, generalized hypotonia, mild dystonia, oculogyric crisis, only babbling	IVS6 + 4A>T/IVS6 + 4A>T	No uptake
6	15	M	Developmental delay, generalized hypotonia, generalized dystonia, oculogyric crisis, only cooing	IVS6 + 4A>T/IVS6 + 4A>T	No uptake
7	15	F	Developmental delay, generalized hypotonia, paroxysmal dystonia, seizure episodes, oculogyric crisis, excessive sweating, only babbling	IVS6 + 4A>T/c1298-1299InsA	Not done
8	21	F	Developmental delay, generalized hypotonia, mild dystonia, oculogyric crisis, sleep problem, excessive sweating, only babbling and cooing	IVS6 + 4A>T/IVS6 + 4A>T	No uptake
9	23	M	Developmental delay, generalized hypotonia, oculogyric crisis, sleep problem, excessive sweating, babbling and cooing, no single words	c1298-1299InsA/-	Trace uptake in bilateral basal ganglion
10	33	M	Developmental delay, generalized hypotonia, dystonia, oculogyric crisis, only babbling and cooing, no single word	IVS6 + 4A>T/IVS6 + 4A>T	Not done
11	38	M	Developmental delay, mild dystonia, oculogyric crisis, sleep problem, excessive sweating, only babbling and cooing, no single word	c236A>G/IVS6 + 4A>T	No uptake
12	50	F	Developmental delay, generalized hypotonia, oculogyric crisis, only babbling, no single word	IVS6 + 4A>T/IVS6 + 4A>T	Not done

Using TBSS approach, we further evaluated the changes in major fiber tracts. After Bonferroni correction, it revealed significantly increased radial and axial diffusivity and decreased FA in some major fiber tracts, which were most evident in arcuate tract, superior longitudinal fasciculus, inferior longitudinal fasciculus, anterior corona radiate, anterior cingulate, frontostriatal white matter, anterior and posterior limbs of the internal capsule, and cerebral peduncle (Table III; Fig. 2). Most of them were related to motor function and language function.

DISCUSSION

AADC is widely distributed in the brain parenchyma, including the substantia nigra and cerebral cortex [Ichinose et al., 1994; Levitt et al., 1997], and is responsible for the decarboxylation step in the monoamine biosynthesis [Lee et al., 2009b]. AADC deficiency will therefore decrease the synthesis of biogenic monoamines, including dopamine, norepinephrine, epinephrine, and serotonin [Lee et al., 2009a, b; Shih et al., 2013]. Dopamine, serotonin

TABLE II. Ratios measured at the frontal lobes, caudate nuclei and corpus callosum in study and control subjects

	FI ratio[a]	Thickness of frontal horn	Width of head of caudate nucleus	FC ratio[b]	Volume of the caudate nucleus	SG ratio[c]
Study group	0.97 ± 0.03	0.60 ± 0.12	0.78 ± 0.11	0.66 ± 0.26	2.15 ± 0.62	1.21 ± 0.36
CI	0.02	0.11	0.06	0.14	0.34	0.20
Control group	0.99 ± 0.02	0.28 ± 0.15	1.00 ± 0.11	0.28 ± 0.15	2.71 ± 0.59	0.86 ± 0.23
CI	0.01	0.09	0.07	0.09	0.36	0.14
P value	0.47	<0.01	<0.01	<0.01	0.02	<0.01

[a]FI ratio = ratio of the transverse diameter of both frontal lobes to the distance between inner tables of both frontal calvarium.
[b]FC ratio = ratio of the thickness of the left frontal horn to the caudate nucleus.
[c]SG ratio = ratio of the thickness of the splenium to that of the genu of the corpus callosum; CI = 95% confidence interval.

and norepinephrine/epinephrine all play important roles in neuronal development and modulation [Gaspar et al., 2003; Shih et al., 2013; Zhou et al., 1995]. AADC deficiency may therefore lead to motor, behavioral, and cognitive dysfunction. Previous study using ^{18}F-Dopa PET in patients with AADC deficiency had disclosed remarkably reduced dopamine biosynthesis in the striatum [Hsieh et al., 2005; Lee et al., 2009a]. In our study, most patients with AADC deficiency did not disclose uptake of ^{18}F-Dopa, and only one patient revealed trace uptake in striatum, indicating reduced AADC activity in brain.

Although previous MRI and MRS studies suggested that patients with AADC deficiency usually have normal or very mild abnormality in MRI [Brun et al., 2010; Lee et al., 2009b; Pons et al., 2004], our present study using age-matched controls revealed that patients with AADC deficiency usually have abnormal brain development, including atrophy of the central and peripheral cerebral parenchyma, prominent subarachnoid spaces overlying both frontal lobes, and hypomyelination. The AADC patients also had significantly widened frontal horns and smaller caudate nuclei, leading to the significant increase

TABLE III. Cerebral diffusion tensor indices of the AADC patients as compared with the age-matched controls using TBSS approach

		EV1	EV2	EV3	ADC	FA
Arcuate tract	Patient	1.467 ± 0.345	1.123 ± 0.268	0.620 ± 0.340	3.284 ± 0.886	0.416 ± 0.123
	Control	1.148 ± 0.239	0.802 ± 0.086	0.347 ± 0.083	2.342 ± 0.280	0.501 ± 0.085
		**	***	*	***	NS
Inferior longitudinal fasciculus	Patient	1.606 ± 0.267	1.183 ± 0.258	0.633 ± 0.362	3.450 ± 0.773	0.499 ± 0.301
	Control	1.274 ± 0.224	0.939 ± 0.158	0.329 ± 0.133	2.324 ± 0.634	0.579 ± 0.058
		***	**	**	***	***
Anterior cingulate	Patient	1.456 ± 0.309	1.158 ± 0.299	0.760 ± 0.399	3.292 ± 0.855	0.358 ± 0.121
	Control	1.249 ± 0.271	0.893 ± 0.098	0.348 ± 0.127	2.467 ± 0.402	0.504 ± 0.110
		NS	***	***	***	**
Anterior corona radiata	Patient	1.666 ± 0.285	1.172 ± 0.285	0.488 ± 0.279	3.301 ± 0.890	0.526 ± 0.12
	Control	1.413 ± 0.333	0.857 ± 0.118	0.195 ± 0.120	2.374 ± 0.277	0.606 ± 0.078
		***	***	*	***	NS
Superior longitudinal fasciculus	Patient	1.659 ± 0.416	1.065 ± 0.342	0.350 ± 0.171	3.296 ± 0.853	0.473 ± 0.065
	Control	1.385 ± 0.284	0.768 ± 0.101	0.200 ± 0.143	2.444 ± 0.434	0.584 ± 0.106
		NS	**	***	***	***
Frontostriatal	Patient	1.511 ± 0.314	1.181 ± 0.286	0.666 ± 0.366	3.317 ± 0.813	0.378 ± 0.128
	Control	1.285 ± 0.312	0.875 ± 0.139	0.367 ± 0.158	2.508 ± 0.362	0.545 ± 0.065
		NS	***	***	***	***
Anterior limb of internal capsule	Patient	1.439 ± 0.274	1.009 ± 0.243	0.499 ± 0.235	2.978 ± 0.675	0.476 ± 0.081
	Control	1.258 ± 0.207	0.764 ± 0.158	0.227 ± 0.141	2.233 ± 0.429	0.592 ± 0.121
		NS	***	***	***	**
Posterior limb of internal capsule	Patient	1.758 ± 0.471	0.817 ± 0.219	0.297 ± 0.219	2.714 ± 0.628	0.706 ± 0.103
	Control	1.336 ± 0.297	0.680 ± 0.161	0.105 ± 0.120	2.172 ± 0.370	0.726 ± 0.111
		***	NS	**	***	NS
Cerebral peduncle	Patient	1.797 ± 0.344	0.984 ± 0.313	0.472 ± 0.291	3.213 ± 0.801	0.632 ± 0.140
	Control	1.478 ± 0.593	0.775 ± 0.154	0.181 ± 0.172	2.327 ± 0.560	0.752 ± 0.129
		**	NS	***	***	**

NS: not significant; *: Bonferroni-adjusted P value < 0.05; **: Bonferroni-adjusted P value < 0.01; ***: Bonferroni-adjusted P value < 0.001.

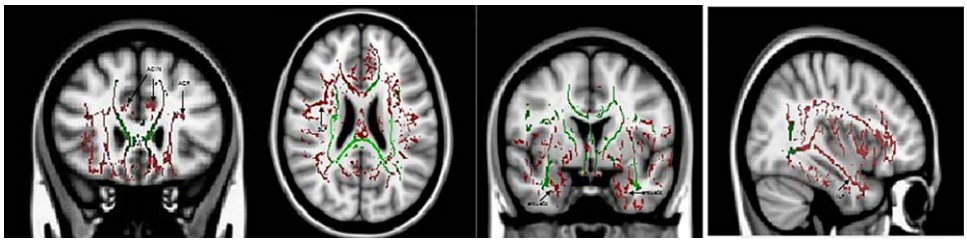

Figure 2.

DTI analysis using TBSS approach in patients with AADC deficiency. It showed significantly decreased FA in anterior corona radiata (ACR), arcuate fascicle (arcuate), anterior cingulate fascicle (ACIN), inferior longitudinal fasciculus (ILF), and superior longitudinal fascicle (SLF) in addition those related to motor function. Red pixels = tracts with significant difference between AADC patients and control subjects ($P < 0.05$); green lines = FA skeleton on the template of a control subject. [Color figure can be viewed at wileyonlinelibrary.com]

of FC ratios. Prominent frontal horns are a nonspecific finding and can be related to decrease of central frontal white matters [Thompson et al., 2006], small striatum, or obstruction of the CSF flow. In our study, the volume of the caudate nucleus in patients with AADC deficiency was significantly smaller than that of the controls. Follow-up MRI also revealed progressive decrease of the volume of caudate nucleus in one patient and decrease of the putamen in another patient. It indicated that deficiency of AADC may influence the development of striatum, and also lead to progressive atrophy of striatum.

In the present study, the genu of the corpus callosum was thinner than the splenium in AADC deficiency patients, leading to the significant increase of SG ratios in the patients. Studies of the morphology and projections of the corpus callosum suggest that the genu of corpus callosum mainly projects to prefrontal cortex [Abe et al., 2004; De Lacoste et al., 1985], and is related to cognition and other frontal lobe function. Therefore, atrophic changes in genu of corpus callosum may be expected to correspond to frontal cortical atrophy in patients with AADC deficiency. There are three main dopaminergic pathways in the brain, and one of these, the mesocortcial pathway, projects from the ventral tegmental area to the frontal cortex. Therefore, AADC deficiency may thus affect the frontal lobe function, leading to the decrease of frontal white matters, dilatation of frontal horn, and atrophy of corpus callosum genu.

To further evaluate the effect of AADC deficiency on fiber tract development, we use FDI and DTI to evaluate the white matter development in the patients. FDI represents the average number of reconstructed fibers passing through the voxel, and had been introduced as a measure to quantify white matter fiber attenuation [Haas et al., 2012; Roberts et al., 2005; Ukmar et al., 2012]. Previous studies had showed that FDI can characterize white matter pathology. FDI can therefore be used to estimate the number of intact white matter tracts in neurological diseases [Ukmar et al., 2012]. DTI indices, including FA, are sensitive to disclose the white matter abnormalities which are not always associated with volume loss of white matter tracts [Duning et al., 2010]. In our study, we showed that most major fiber tract in the brain of AADC patients had reduced FDI, indicating the reduced biosynthesis of dopamine and serotonin in AADC deficiency may affect the development of white matter. To further clarify the major changes in fiber tracts, we used TBSS approaches to investigate the most significant difference in fiber tracts. We found that the most significant changes in fiber tracts were in arcuate tract, inferior longitudinal fasciculus, anterior cingulate bundle, anterior corona radiate, and superior longitudinal fasciculus in addition to those related to motor function. It is suggested that there are dorsal and ventral pathways for language [Saur et al., 2008]. The dorsal route involved superior longitudinal fascicle, arcuate fascicle, and middle longitudinal fascicle. The ventral route, associated with sentence comprehension, comprised of middle longitudinal fascicle, the extreme capsule and the inferior longitudinal fascicle. Damage to inferior longitudinal fascicle, arcuate fasciculus and superior longitudinal fasciculus-related pathways could thus induce deficits in object naming, phonological language function and writing, respectively [Mandonnet et al., 2007; Saur et al., 2008; Shinoura et al., 2013]. Recent studies had also shown impaired neural connectivity in the corpus callosum/cingulum and temporal lobes involving the inferior longitudinal fasciculus and superior longitudinal fasciculus in children with autistic spectrum disorders [Aoki et al., 2013; Jou et al., 2011]. Children with AADC deficiency usually have great impairment in language and social perception as shown in our study. They may also present with autistic behavior in those with mild neurological symptoms [Brun et al., 2010; Lee et al., 2009b]. In our study, five patients (one older than 1 year) only had cooing, and did not develop babbling in speech. For those over 1 year, no one can speak words or phrases with significant meaning. It indicated the possibility of impairment of the language pathways in addition to motor pathways

in children with AADC deficiency, which was compatible with the present findings in DTI studies. Preliminary report in gene therapy for AADC deficiency showed improved motor function without prominent improvement in language function, which also supported the possible involvement of language pathways in these patients [Hwu et al., 2012]. Further long-term follow-up of the language development of these patients may clarify their relationship with the defects in these fiber tracts.

In our present study, anterior cingulate bundle also showed reduced FA. The anterior cingulate cortex–striatum pathway plays an important role in information integration. It can receive information from limbic system and sends information to other motor areas, and can be associated with emotion and other cognitive functions [Allman et al., 2001]. Severe white matter loss in the right frontal lobe, including the anterior cingulate, had been found in depressed Parkinson disease patients [Kostić and Filippi, 2011]. Because dopamine is the major neurotransmitter that can modulate the cortical–basal ganglia loop [Kostić and Filippi, 2011; Parent and Hazrati, 1995], dopamine deficiency secondary to AADC deficiency can therefore affect the function of anterior cingulate.

In our study, three patients with follow-up MRI also revealed progressive mesiotemporal atrophy and decrease of subcortical and perventricular white matter in follow-up MRI, indicating that AADC deficiency may lead to progressive cerebral atrophy. There are several potential factors leading to the progressive cerebral atrophy in AADC deficiency. In addition to the negative effect of deficiency of biogenic monoamines and serotonin on brain development, the accumulation of L-dopa due to AADC deficiency or dopamine agonist treatment may be toxic to the neurons [Asanuma et al., 2003; Anselm and Darras, 2006; Jenner and Brin, 1998]. Although episodic hypoglycemia or instability of cardiovascular system may predispose the patients to significant cerebral damage [Anselm and Darras, 2006; Brun et al., 2010; Lee et al., 2009a], there was no evident hypoglycemic brain injury in MRI. Therefore, serial follow-up brain MRI in more patients with AADC deficiency may clarify the possible factors leading to the progressive changes in MRI.

CONCLUSION

Although previous studies did not reveal significant effect of AADC deficiency on the brain, the MR findings in the present study indicated that AADC deficiency may have great impact on brain development, especially over frontal lobe and fiber tracts related to cognition and language function. The mildly progressive cerebral atrophy may arise from neurotransmitter deficiency or side effect of drug treatment. Long-term follow-up of neuroimaging findings in patients with AADC deficiency may provide more evidences of the effect of AADC deficiency on brain development.

ACKNOWLEDGMENTS

The authors thank Professor Wen-Chung Lee in Institute of Epidemiology and Preventive Medicine in the College of Public Health, National Taiwan University, for assistance in statistical analysis.

REFERENCES

Abe O, Masutani Y, Aoki S, Yamasue H, Yamada H, Kasai K, Mori H, Hayashi N, Masumoto T, Ohtomo K (2004): Topography of the human corpus callosum using diffusion tensor tractography. J Comput Assist Tomogr 28:533–539.

Allman JM, Hakeem A, Erwin JM, Nimchinsky E, Hof P (2001): The anterior cingulate cortex. The evolution of an interface between emotion and cognition. Ann N Y Acad Sci 935: 107–117.

Anselm IA, Darras BT (2006): Catecholamine toxicity in aromatic L-amino acid decarboxylase deficiency. Pediatr Neurol 35: 142–144.

Aoki Y, Abe O, Nippashi Y (2013): Comparison of white matter integrity between autism spectrum disorder subjects and typically developing individuals: A meta-analysis of diffusion tensor imaging tractography studies. Mol Autism 4:25.

Asanuma M, Miyazaki I, Ogawa N (2003): Dopamine- or L-DOPA-induced neurotoxicity: The role of dopamine quinone formation and tyrosinase in a model of Parkinson's disease. Neurotox Res 5:165–176.

Barkovich AJ (2000): Concepts of myelin and myelination in neuroradiology. AJNR Am J Neuroradiol 21:1099–1109.

Barkovich AJKB, Jackson DEJ, Norman D (1988): Normal maturation of the neonatal and infant brain: MR imaging at 1.5 T. Radiology 166:173–180.

Behrens TE, Berg HJ, Jbabdi S, Rushworth MF, Woolrich MW (2007): Probabilistic diffusion tractography with multiple fibre orientations. What can we gain?. NeuroImage 34:144–155.

Brun L, Ngu LH, Keng WT, Ch'ng GS, Choy YS, Hwu WL, Lee WT, Willemsen MA, Verbeek MM, Wassenberg T, Régal L, Orcesi S, Tonduti D, Accorsi P, Testard H, Abdenur JE, Tay S, Allen GF, Heales S, Kern I, Kato M, Burlina A, Manegold C, Hoffmann GF, Blau N (2010): Clinical and biochemical features of aromatic L-amino acid decarboxylase deficiency. Neurology 75:64–71.

De Lacoste MC, Kirkpatrick JB, Ross ED (1985): Topography of the human corpus callosum. J Neuropathol Exp Neurol 44: 578–591.

Duning T, Kellinghaus C, Mohammadi S, Schiffbauer H, Keller S, Ringelstein EB, Knecht S, Deppe M (2010): Individual white matter fractional anisotropy analysis on patients with MRI negative partial epilepsy. J Neurol Neurosurg Psychiatry 81: 136–139.

Fan S, van den Heuvel OA, Cath DC, van der Werf YD, de Wit SJ, de Vries FE, Veltman DJ, Pouwels PJ (2016): Mild white matter changes in un-medicated obsessive-compulsive disorder patients and their unaffected siblings. Front Neurosci 9:495.

Gaspar P, Cases O, Maroteaux L (2003): The developmental role of serotonin: News from mouse molecular genetics. Nat Rev Neurosci 4:1002–1012.

Haas BW, Hoeft F, Barnea-Goraly N, Golarai G, Bellugi U, Reiss AL (2012): Preliminary evidence of abnormal white matter related to the fusiform gyrus in Williams syndrome: A

diffusion tensor imaging tractography study. Genes Brain Behav 11:62–68.

Hsieh HJ, Lin SH, Liu HM (2005): Visualisation of impaired dopamine biosynthesis in a case of aromatic L-amino acid decarboxylase deficiency by co-registered ^{18}F FDOPA PET and magnetic resonance imaging. Eur J Nucl Med Mol Imaging 32: 517.

Hwu WL, Muramatsu S, Tseng SH, Tzen KY, Lee NC, Chien YH, Snyder RO, Byrne BJ, Tai CH, Wu RM (2012): Gene therapy for aromatic L-amino acid decarboxylase deficiency. Sci Transl Med 4:134ra61.

Ichinose H, Ohye T, Fujita K, Pantucek F, Lange K, Riederer P, Nagatsu T (1994): Quantification of mRNA of tyrosine hydroxylase and aromatic L-amino acid decarboxylase in the substantia nigra in Parkinson's disease and schizophrenia. J Neural Transm Park Dis Dement Sect 8:149–158.

Jenner PG, Brin MF (1998): Levodopa neurotoxicity: Experimental studies versus clinical relevance. Neurology 50:S39–S43.

Jiang H, van Zijl PC, Kim J, Pearlson GD, Mori S (2006): DtiStudio: Resource program for diffusion tension computation and fiber bundle tracking. Comput Meth Prog Biomed 81:106–116.

Jou RJ, Jackowski AP, Papademetris X, Rajeevan N, Staib LH, Volkmar FR (2011): Diffusion tensor imaging in autism spectrum disorders: Preliminary evidence of abnormal neural connectivity. Aust N Z J Psychiatry 45:153–162.

Jovicich J, Marizzoni M, Bosch B, Bartrés-Faz D, Arnold J, Benninghoff J, Wiltfang J, Roccatagliata L, Picco A, Nobili F, Blin O, Bombois S, Lopes R, Bordet R, Chanoine V, Ranjeva JP, Didic M, Gros-Dagnac H, Payoux P, Zoccatelli G, Alessandrini F, Beltramello A, Bargalló N, Ferretti A, Caulo M, Aiello M, Ragucci M, Soricelli A, Salvadori N, Tarducci R, Floridi P, Tsolaki M, Constantinidis M, Drevelegas A, Rossini PM, Marra C, Otto J, Reiss-Zimmermann M, Hoffmann KT, Galluzzi S, Frisoni GB, PharmaCog Consortium (2014): Multisite longitudinal reliability of tract-based spatial statistics in diffusion tensor imaging of healthy elderly subjects. Neuroimage 101:390–403.

Kostić VS, Filippi M (2011): Neuroanatomical correlates of depression and apathy in Parkinson's disease: Magnetic resonance imaging studies. J Neurol Sci 310:61–63.

Lee WT, Weng WC, Peng SF, Tzen KY (2009a): Neuroimaging findings in children with paediatric neurotransmitter diseases. J Inherit Metab Dis 32:361–370.

Lee HF, Tsai CR, Chi CS, Chang TM, Lee HJ (2009b): Aromatic L-amino acid decarboxylase deficiency in Taiwan. Eur J Paediatr Neurol 13:135–140.

Levitt P, Harvey JA, Friedman E, Simansky K, Murphy EH (1997): New evidence for neurotransmitter influences on brain development. Trends Neurosci 20:269–274.

Mandonnet E, Nouet A, Gatignol P, Capelle L, Duffau H (2007): Does the left inferior longitudinal fasciculus play a role in language? A brain stimulation study. Brain 130:623–629.

Parent A, Hazrati LN (1995): Functional anatomy of the basal ganglia. I. The cortico-basal ganglia-thalamo-cortical loop. Brain Res Brain Res Rev 20:91–127.

Pons R, Ford B, Chiriboga CA, Clayton PT, Hinton V, Hyland K, Sharma R, De Vivo DC (2004): aromatic L-amino acid decarboxylase deficiency: Clinical features, treatment and prognosis. Neurology 62:1058–1065.

Roberts TP, Liu F, Kassner A, Mori S, Guha A (2005): Fiber density index correlates with reduced fractional anisotropy in white matter of patients with glioblastoma. AJNR Am J Neuroradiol 26:2183–2186.

Saur D, Kreher BW, Schnell S, Kümmerer D, Kellmeyer P, Vry MS, Umarova R, Musso M, Glauche V, Abel S, Huber W, Rijntjes M, Hennig J, Weiller C (2008): Ventral and dorsal pathways for language. Proc Natl Acad Sci U S A 105:18035–18040.

Schiffmann R, van der Knaap MS (2009): Invited article: An MRI-based approach to the diagnosis of white matter disorders. Neurology 72:750–759.

Shih DF, Hsiao CD, Min MY, Lai WS, Yang CW, Lee WT, Lee SJ (2013): Aromatic L-amino acid decarboxylase (AADC) is crucial for brain development and motor functions. PLoS One 8: e71741.

Shinoura N, Midorikawa A, Onodera T, Tsukada M, Yamada R, Tabei Y, Itoi C, Saito S, Yagi K (2013): Damage to the left ventral, arcuate fasciculus and superior longitudinal fasciculus-related pathways induces deficits in object naming, phonological language function and writing, respectively. Int J Neurosci 123:494–502.

Smith SM, Jenkinson M, Woolrich MW, Beckmann CF, Behrens TE, Johansen-Berg H, Bannister PR, De Luca M, Drobnjak I, Flitney DE, Niazy RK, Saunders J, Vickers J, Zhang Y, De Stefano N, Brady JM, Matthews PM (2004): Advances in functional and structural MR image analysis and implementation as FSL. NeuroImage 23(S1):208–219.

Smith SM, Jenkinson M, Johansen-Berg H, Rueckert D, Nichols TE, Mackay CE, Watkins KE, Ciccarelli O, Cader MZ, Matthews PM, Behrens TE (2006): Tract-based spatial statistics: Voxelwise analysis of multi-subject diffusion data. NeuroImage 31:1487–1505.

Thompson PM, Dutton RA, Hayashi KM, Lu A, Lee SE, Lee JY, Lopez OL, Aizenstein HJ, Toga AW, Becker JT (2006): Mapping of ventricular and corpus callosum abnormalities in HIV/AIDS. Neuroimage 31:12–23.

Ukmar M, Montalbano A, Makuc E, Specogna I, Bratina A, Longo R, Cova MA (2012): Fiber density index in the evaluation of the spinal cord in patients with multiple sclerosis. Radiol Med 117:1215–1224.

Woolrich MW, Jbabdi S, Patenaude B, Chappell M, Makni S, Behrens T, Beckmann C, Jenkinson M, Smith SM (2009): Bayesian analysis of neuroimaging data in FSL. NeuroImage 45: S173–S186.

Xu D, Mori S, Solaiyappan M, van Zijl PC, Davatzikos C (2002): A framework for callosal fiber distribution analysis. NeuroImage 17:1131–1143.

Yamada H, Sadato N, Konishi Y, Muramoto S, Kimura K, Tanaka M, Yonekura Y, Ishii Y, Itoh H (2000): A milestone for normal development of the infantile brain detected by functional MRI. Neurology 55:218–223.

Zhou QY, Qualfe CJ, Palmiter RD (1995): Targeted disruption of the tyrosine hydroxylase gene reveals that catecholamines are required for mouse fetal development. Nature 374:640–643.